Remote Sens. **2015**, *7*, 9292-9310; doi:10.3390/rs70709292

OPEN ACCESS

remote sensing

ISSN 2072-4292

www.mdpi.com/journal/remotesensing

Article

Joint Quality Measure for Evaluation of Pansharpening Accuracy

Gintautas Palubinskas

Remote Sensing Technology Institute, German Aerospace Center (DLR), Oberpfaffenhofen, 82234 Wessling, Germany; E-Mail: Gintautas.Palubinskas@dlr.de;
Tel.: +49-8153-28-1490; Fax: +49-8153-28-1444.

Academic Editors: Giles Foody, Josef Kellndorfer and Prasad S. Thenkabail

Received: 17 April 2015 / Accepted: 9 July 2015 / Published: 21 July 2015

Abstract: A new Joint Quality Measure (JQM), which is a sole measure, is proposed for quality ranking of pansharpening methods. It is based on a newly proposed Composite similarity measure, which consists of Means, Standard deviations and Correlation coefficient (CMSC), and is translation invariant with respect to means and standard deviations. The JQM itself consists of a weighted sum of two terms. The first term is measured between a low pass filtered pansharpened image and original multispectral image at a reduced/low resolution scale. The second term is measured between the intensity calculated from spectrally weighted pansharpened multispectral image and original panchromatic image in a high resolution scale. Experimental results show advantages of a new measure, JQM, for quality assessment of pansharpening methods on the one hand, and drawbacks or unexpected properties of the already known measure, Quality with No Reference (QNR), on the other hand.

Keywords: image fusion; multi-resolution; low pass filtering; quality assessment; similarity measure

1. Introduction

Pansharpening aims to include spatial/detail information from a high resolution image into a low resolution image while preserving spectral properties of a low resolution image. For example, a high resolution image is a panchromatic/multispectral image, and a low resolution image is a multi-spectral/hyper-spectral image. A large number of algorithms and methods to solve this problem were introduced during the last two decades, which can be divided into two main groups. The first group

of methods is based on a linear spectral transformation, e.g., Intensity-Hue-Saturation (IHS), Principal Component Analysis, and Gram-Schmidt orthogonalization (GS), followed by a Component Substitution (CS). Methods of the second group use spatial frequency decomposition usually performed by means of high pass filtering, e.g., boxcar filter in signal domain, filtering in Fourier domain or Multi-Resolution Analysis (MRA) using wavelet transform. Here I have to mention that there are some attempts to combine both types of methods. Moreover, there exist a group of methods which state the pansharpening task as an ill-posed recovery problem solved by regularization using Bayesian estimation and recently proposed sparse representation approaches. For recent surveys of various image fusion methods see publications [1–4].

In parallel to the development of pansharpening methods, many attempts were undertaken to assess quantitatively their quality usually using measures originating from signal/image processing such as Mean Squared Error (MSE), Peak Signal-to-Noise Ratio (PSNR), relative dimensionless global error in synthesis (ERGAS), Pearson's Correlation Coefficient (CC), Spectral Angle Mapper (SAM), Universal Image Quality Indices (UIQI/SSIM) and their multispectral extensions ($Q4/Q2^n$). For recent overviews of quality measures, see references [5,6]. These simple/separate measures defined in scalar/vector form can be used only as Full Reference (FR) measure, that is, when the reference image is available. This situation is valid for quite few applications mostly simulations. Due to the missing reference in pansharpening quality assessment task different solutions or so-called protocols were proposed: Wald's protocol [7], Zhou's protocol [8], Quality with No Reference (QNR) [9] and Khan's protocol [10], which usually include the calculation of several quality measures. Of course, a sole or joint quality measure, as already proposed in [9,11,12], enables much easier and practical/comfortable ranking of various fusion methods.

Usually pansharpening in image processing is used to increase visual quality of an image. In remote sensing, this task is fully different because it aims at enhancing image quality for further processing such as clustering, classification, matching and change detection thus requiring only relative comparison of data (so-called image value/intensity translation invariant applications). For example, the quality measure UIQI/SSIM [13] was designed for perceptual tasks or scale invariant applications, but recently it is spreading widely in other applications. Thus, its usage in pansharpening quality assessment in remote sensing imagery, e.g., QNR [9] and joint quality measures [11,12], can lead to wrong results. Because MSE and UIQI/SSIM based measures are not very suitable for translation invariant with respect to sample means and standard deviations applications [14], I propose to exchange/replace the above-mentioned UIQI/SSIM measures with a new measure—composite measure—based on means, standard deviations and correlation coefficient (CMSC) [14], which is translation invariant with respect to means and standard deviations, thus enhancing measures proposed in [12].

In this paper, I perform a comparison of six pansharpening methods originating from the main earlier mentioned groups of methods and several parameter settings using a new joint quality measure (JQM) and already known measure of QNR for IKONOS and WorldView-2 satellite data.

2. Quality Assessment Measures

In this section, I will review/summarize several possible ways and strategies to assess the quality of pansharpening methods and additionally introduce a new joint quality measure.

2.1. Full Reference Measures

Quality or similarity measures can be divided into two main groups: Full reference measures when the reference image is existent and no reference measures. The latter case is more frequent because in most applications the reference is missing. Examples of FR measures (scalar or vector based) used to assess pansharpening quality are SAM, MSE and measures based on it, e.g., PSNR, Relative Average Spectral Error (RASE) and ERGAS, CC, universal image quality indices (UIQI/SSIM) and multispectral extensions of UIQI (Q4/Q2^n) just to mention few or most popular of them. Deep understanding of the properties of distance or similarity measures is important in order to use them correctly in a particular application. Perhaps the two most important properties of the distance measures are: Translation invariance

$$d(p_1 + c, p_2 + c) = d(p_1, p_2) \tag{1}$$

and scale invariance

$$d(c \cdot p_1, c \cdot p_2) = d(p_1, p_2) \tag{2}$$

defined for all variables/parameters p_i and some fixed constant c. From Equation (1) follows directly

$$d(p, p + c) = \text{constant} \tag{3}$$

for all p and some fixed c, which means that translation invariance implies an independence of the measure on the absolute parameter values or equivalently dependence only on the relative relation, e.g., difference of the parameters. For example, correlation coefficient is both translation and scale invariant with respect to original data values x, y. Thus, the selection of a particular measure is application dependent. For example for image matching, clustering or classification applications translation invariant measures such as MSE can be more suitable. For visual perception applications scale invariant measures such as UIQI/SSIM are preferable.

It was shown in [14] that MSE based measures are not translation invariant with respect to sample standard deviation. The recently widely spreading UIQI/SSIM measure is not translation invariant with respect to both sample moments—means and standard deviations. This can lead to false quality assessment results in applications such as classification, clustering, matching and change detection, which usually require translation invariance property Equation (1) or equivalently only relative comparison of parameters independent of their absolute values Equation (3). Pansharpening products in remote sensing are mostly used for further processing in the above-mentioned applications. Thus, a new quality measure CMSC, which is translation invariant with respect to means and standard deviations [14], can be more suitable/justified

$$CMSC(x, y) = (1 - d_1) \cdot (1 - d_2) \cdot \rho, \;\; d_1 = \frac{(\mu_x - \mu_y)^2}{R^2}, \;\; d_2 = \frac{(\sigma_x - \sigma_y)^2}{(R/2)^2}, \tag{4}$$

where $\mu_{x,y}$ and $\sigma_{x,y}$ are means and standard deviations for two signal/image patches x, y; ρ is Pearson's correlation coefficient and $R = 2^8 - 1 = 255$ for 8bit data.

I have to note that there exist some attempts to measure image quality without reference mostly based on gradients in an image [15]. However, they are not sensitive/subtle enough to measure fine differences that usually occur during pansharpening processes. Thus, the following practical approaches have been established over the past two decades and are presented in the following Section 2.3.

2.2. Application Based Quality Assessment

As the reference image is not available in pansharpening applications an ideal or objective way to assess quality of pansharpening products would be to evaluate their impact in a particular application by using reference/ground truth data of a given application. This way is very time- and resource-consuming and is thus is not practical in the selection of a suitable method from the hundreds of methods available [3].

2.3. Quality Assessment Based on Comparison with Input Data

A practical way of quality assessment is based on the comparison of a fusion result with the two inputs of pansharpening: Low resolution multispectral image ms_k (k is the index of the spectral band) and high resolution panchromatic image *pan*.

2.3.1. Quality Assessment Based on an Original Multispectral Image at Low Resolution Scale

For this type of comparison, the following two approaches have been established during the two past decades.

In the first approach, the multispectral fusion result msf_k in a high resolution scale is compared with the original multispectral image ms_k, which is available at a low resolution scale. This is so that the high resolution pansharpened image should be low pass filtered and decimated to the resolution of original multispectral image. This way of pansharpening quality assessment is known as a consistency or Wald's protocol first property [7,16]. Any FR measure mentioned in Section 2.1 can be used for this purpose. Usually, the cutoff frequency of a low pass filter is equal to the ratio of high resolution to low resolution. In Khan's protocol [10], the cutoff frequencies of low pass filters are derived from instrument based spectral Modulation Transfer Functions (MTFs).

The recently proposed spectral distortion measure D_λ, which is a one part of QNR protocol [9], avoids preprocessing of the fused result by comparing inter-band UIQI values separately calculated at different resolutions

$$D_\lambda = \frac{1}{N \cdot (N-1)} \sum_{l,k=1}^{N} \left| UIQI(ms_l, ms_k) - UIQI(msf_l, msf_k) \right| \tag{5}$$

where N is the number of bands. Unfortunately, evidence or proof that such inter-band relations hold between resolution scales is not provided or missing. Moreover, such inter-band comparison of different spectral bands is possible mathematically, but is incorrect physically because different parts of spectrum or more generally content/information are compared which may be incommensurable.

I propose to enhance the Quality measure at Low Resolution (QLR) proposed in [12] by replacing the SSIM with a newly introduced CMSC Equation (4) [14] and additionally including sensor spectral response function gains to account for different spectral overlap of multispectral and panchromatic bands. Thus, QLR is defined in a reduced resolution space and compares only multispectral images which are spectrally overlapping with the panchromatic band

$$QLR = \sum_{k=1}^{N} w_k \cdot CMSC(ms_k, msf_{k,lpf}) \tag{6}$$

where w_k—spectral response weight for band k, which is calculated from spectral response functions of data provider [17], $msf_{k,lpf} = (msf_k * lpf_k)\downarrow$, lpf_k—a Gaussian low pass filter which can be band dependent, *—convolution operator, ↓ means decimating of high resolution data to a low resolution scale. Thus, two new enhancements of [12] are introduced: A new FR measure CMSC and the spectral weights w_k. Moreover, this measure is spectrally consistent or physically correct in that sense that it compares the commensurable information or the same parts (bands) of electromagnetic spectrum.

In the second approach proposed by Wald [7,16] also known as a synthesis property (Wald's protocol second and third property) a fused multi-band result is compared with a reference in high resolution separately for each band and using inter-band relations. Due to the missing reference at high resolution the following preprocessing of data to reduced resolution scale is performed. Input data ms_k and *pan* are low pass filtered and decimated by a factor equal to the resolution scale ratio of *pan* to ms_k images: $ms_{k,lpf}$ and pan_{lpf}. Then pansharpening of $ms_{k,lpf}$ using pan_{lpf} is performed. The result of fusion $msf_{k,lpf}$ is compared with original multispectral ms_k images (true reference in this case) using any FR measure mentioned in Section 2.1. Unfortunately, evidence or proof that quality assessment results/conclusions obtained in a reduced resolution scale hold for a high resolution scale is not given or missing.

Measures discussed in this Sub-section estimate the spectral quality of a fusion result (so-called spectral consistency) and are necessary for pansharpening quality assessment. However, they are not sufficient because, e.g., simple nearest neighbor interpolation will outperform all pansharpening methods. Thus, an additional quality assessment in a high resolution scale is necessary to evaluate fusion results correctly.

2.3.2. Quality Assessment based on Panchromatic Image in High Resolution Scale

As already mentioned above, due to the missing reference in the high resolution, only comparison of the fusion result msf_k with the high resolution panchromatic image *pan* can be performed. Usually, this comparison is based on the edge information. In Zhou's protocol, for example, details are extracted using Laplacian filter and then correlation coefficient is used as a quality measure [8]. The recently proposed spatial distortion measure D_s (one part of QNR protocol [9]) compares inter-band UIQI values pair-wise: Between the fused msf_k and the panchromatic image *pan*, and the low resolution multispectral image ms_k and the low pass filtered panchromatic pan_{lpf} image

$$D_s = \frac{1}{N}\sum_{k=1}^{N}\left|UIQI(ms_k, pan_{lpf}) - UIQI(fms_k, pan)\right| \quad (7)$$

where, $pan_{lpf} = pan*lpf$. In Khan's protocol [10] MTF based filters are used to extract high frequency information and the UIQI measure is used for comparison. In [18] MTFs are estimated automatically from the edge information in an image which makes this approach even more practical. Unfortunately, evidence or proof that such comparison of different spectral bands (narrow multispectral band and broad panchromatic band) is legitimate is missing. Moreover, it is incorrect physically or spectrally inconsistent because different spectrum parts or more generally content/information is compared, which may be incommensurable.

Thus, I propose a Quality measure at High Resolution (QHR) which is defined at a high resolution scale [12]. This measure compares the intensity calculated from a weighted sum of multispectral bands (simulated panchromatic image) I_{msf} with the original *pan* image

$$QHR = CMSC(pan, I_{msf}) \tag{8}$$

where

$$I_{msf} = \sum_{k=1}^{N} w_k \cdot msf_k \,. \tag{9}$$

For this measure, QHR, the two new enhancements of [12] are introduced: the new FR measure CMSC and spectral weights w_k calculated from spectral response functions of data provider [17]. This measure is spectrally (physically) consistent because it compares the same portions (bands) of the electromagnetic spectrum. I have to note that this measure includes a check of both spectral and spatial properties of a fusion result. Thus, the following application scenario is possible. For example, if QLR is quite high (good spectral quality) then QHR can be used to compare the spatial quality of a fusion result. Moreover, this measure can act well as a sole measure if no other measures are available because it evaluates both properties of image quality.

2.3.3. Joint Quality Measures based on Both Inputs

Previously, discussed assessment methods (Sections 2.3.1 and 2.3.2) lead to a set of measures derived in low and high resolution scales sometimes called protocols, e.g., Zhou's protocol [8] and Khan's protocol [10]. It is observed that it is quite difficult to rank methods using several measures thus sole or joint measures (produced by averages or products of separate measures) were proposed recently such as QNR [9], product of two measures [11] and JQM [12]. For example, QNR is defined as a product of two separate measures presented in Equations (5) and (7)

$$QNR = (1 - D_\lambda) \cdot (1 - D_s) \tag{10}$$

Whereas JQM is defined as a weighted sum of separate measures presented in Equations (6) and (8)

$$JQM = v_1 \cdot QLR + v_2 \cdot QHR,\ v_1 + v_2 = 1 \tag{11}$$

Equal weights $v_i = 0.5$ are used in this paper. These two joint measures and their corresponding separate measures are employed in this paper to assess quality of pansharpening methods. The ranges of all similarity measures and their compound parts are limited to interval (0, 1) by clipping negative correlation coefficient values to 0 in UIQI and CMSC measures, where one is achieved for identical values.

3. Experimental Results

I will illustrate my ideas concerning pansharpening quality assessment for two optical remote sensing satellites IKONOS and WorldView-2 (WV-2) over Munich, Germany. For scene details see Table 1.

In this section, I will compare six different pansharpening methods (see Section 3.1) and several parameter settings using the proposed JQM and already known QNR joint quality measures, and additionally well-established spectral measures SAM and ERGAS. First, the interpolation influence is only investigated by comparing the four most popular interpolation methods (Section 3.2). Second, the interpolation method influence on one of the pansharpening methods is analyzed in Section 3.3. Finally, the comparison of various pansharpening methods and their parameter settings is presented in Section 3.4.

Table 1. Scene parameters for Ikonos and WorldView-2 data over the city of Munich, Germany.

Sensor Parameter	IKONOS	WorldView-2
Image date	15 July 2005	12 July 2010
Image time (local)	10:28:06	10:30:17
Mode	PAN+MS	PAN+MS
Look angle	5 °Right	5.2 °Left
Product	L2A	L2A
Resolution PAN (m)	1.0	0.5
Resolution MS (m)	4.0	2.0

3.1. Pansharpening Methods

Methods investigated in this paper can be described by the following general expression (see e.g., [1,19,20])

$$msf_k = msi_k + g_k \cdot (pan - pan_{lpf}) \tag{12}$$

where msf_k—fused/pansharpened high resolution multispectral image, k—spectral band number, msi_k—low resolution multispectral image interpolated to a high resolution space, g_k—weight (gain) for detail injection, pan—high resolution panchromatic image and pan_{lpf}—low pass filtered pan image. Usually histogram matching of msf_k and ms_k is performed after application of Equation (12). Then, individual methods can be seen as special cases of Equation (12) as shown below.

General Fusion Filtering (GFF) [21] is defined as

$$msf_k = FFT^{-1}\left[\left(ZP\left(W \cdot FFT\left(ms_k\right)\right) + FFT\left(pan\right) \cdot \left(1 - LPF\right)\right)\right], \tag{13}$$

where $g_k = 1$, ms_k—low resolution multispectral image, ZP—zero padding interpolation, W—Hamming window for ringing artifacts suppression and LPF—low pass filter in Fourier domain.

High Pass Filtering Method HPFM (variant of GFF) [22] is given by

$$msf_k = msi_k + pan - pan_{lpf} \tag{14}$$

with $g_k = 1$, $pan_{lpf} = pan * lpf$, $lpf = FFT^{-1}(LPF)$, where lpf is a Gaussian low pass filter in signal domain. Here, I have to note that the cutoff frequency of a low pass filter can be selected individually for each spectral band as, e.g., already proposed for MRA based methods using modulation transfer function (MTF) information [23].

Ehlers fusion [24] is defined as

$$msf_k = msi_k - I_{msi} + I_{msi} \times lpf\,1 + pan - pan \times lpf\,2 \tag{15}$$

where $g_k = 1$, intensity is defined as

$$I_{msi} = \sum w_k \cdot msi_k \tag{16}$$

w_k are spectral weights calculated from spectral response functions of data provider [17]. Two different low pass filters are used for filtering of pan and intensity images, respectively. Usually original software of the method is not available, thus the author's software implementation is used.

Á trous wavelet transform ATWT [25] is given by Equation (12) with $g_k = 1$ and pan_{lpf}— à trous wavelet decomposed low resolution version of pan. M. Canty's software implementation [26] is used.

Component substitution using IHS transformation (CS IHS) can be written as follows

$$msf_k = msi_k - I_{msi} + pan \quad (17)$$

with $g_k = 1$, $pan_{lpf} = I_{msi}$, and I_{msi} is defined by Equation (16). The author's software implementation is used. Here, I have to note that QHR = 1 for this method what contradicts not to the already known high spatial quality of this method. Thus, usage of an additional measure, e.g., QLR or JQM will allow correctly to discriminate it from other pansharpening methods.

Component substitution using GS transformation (CS GS) is Equation (12) with $pan_{lpf} = I_{msi}$. IDL ENVI 5.0 software implementation is used.

3.2. Interpolation Influence Only

Values of both joint quality measures JQM and QNR and their corresponding separate measures (QLR, QHR and DL, DS) are presented in Figures 1–4 for differently interpolated multispectral data (high resolution scale) of IKONOS (Figures 1 and 2) and WV-2 sensors (Figures 3 and 4). The following interpolation methods are investigated: nearest neighbor (NN), zero padding using Fourier transform (ZP), bilinear interpolation (BIL) and cubic convolution (CUB) (IDL ENVI 5.0 software is used except ZP, which is the author's software implementation).

We see that all interpolation methods exhibit quite similar QLR values for both sensors (Figures 1b and 3b). For example, this is well supported by visual analysis of interpolation results presented in Figure 5. All methods exhibit similar colors or multispectral information. Similarly, all methods have quite similar QHR values except NN. NN has very poor spatial quality. This can be observed in Figure 5a. These results lead to low (poor) values of JQM for NN for both sensors (Figures 1a and 3a). Moderately oscillating values of separate measures QLR and QHR for the other three methods result in slightly higher values of CUB for IKONOS (Figure 1a) and ZP for WV-2 (Figure 3a).

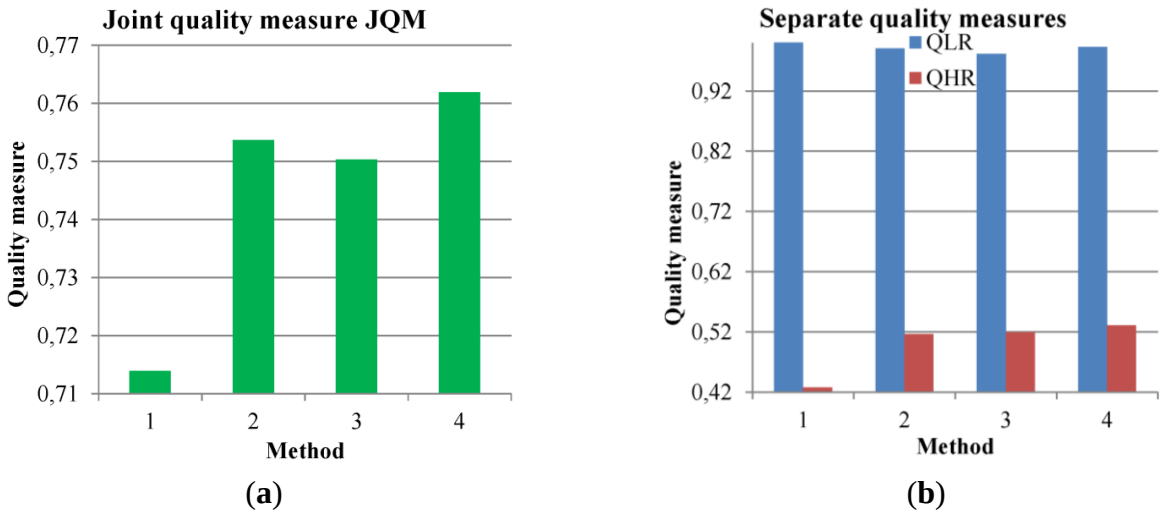

Figure 1. Joint Quality Measure (JQM) quality assessment of interpolation methods: 1—nearest neighbor (NN), 2—zero padding (ZP), 3—bilinear interpolation (BIL), and 4—cubic convolution (CUB) for IKONOS data. (**a**) JQM, (**b**) QLR and QHR.

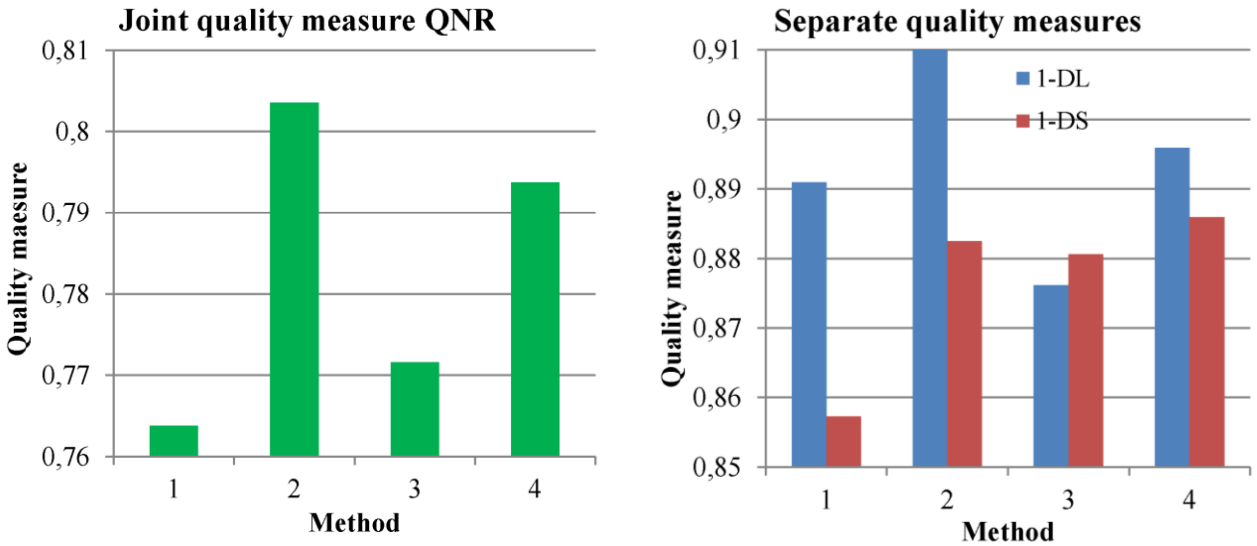

Figure 2. Quality with no Reference (QNR) quality assessment of interpolation methods: 1—NN, 2—ZP, 3—BIL, and 4—CUB for IKONOS data. (**a**) QNR, (**b**) 1−*DL* and 1−*DS*.

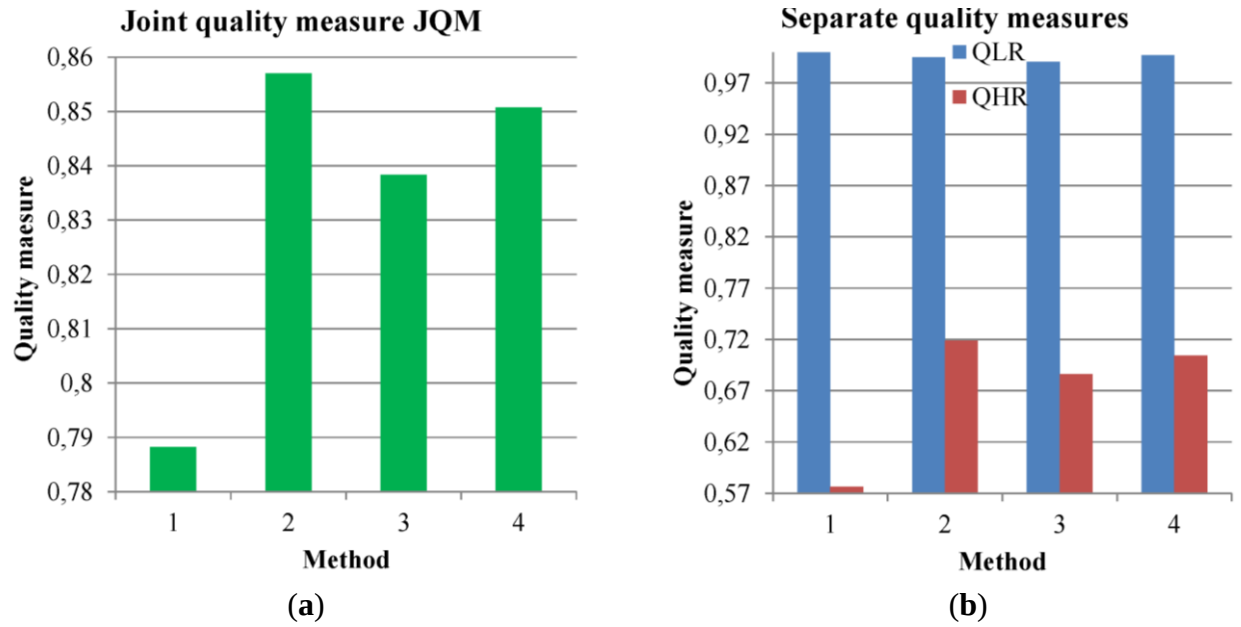

Figure 3. JQM quality assessment of interpolation methods: 1—NN, 2—ZP, 3—BIL, and 4—CUB for WV-2 data. (**a**) JQM, (**b**) QLR and QHR.

The analysis of QNR is more complex due to greater variability of its compound parts. 1−*DL* measure identifies ZP to result in the highest quality, closely followed by CUB. BIL and NN seem to be the worst. Both observations are valid for both sensors (Figures 2b, 4b). 1−*DS* measure (Figure 2b) behaves similarly to QLR (Figure 1b) for IKONOS sensor, but for WV-2 all methods (NN too) seem to be quite similar (Figure 4b). Moreover, the absolute values of this measure are much higher for WV-2 data than for IKONOS. Thus, the QNR value follows approximately the results of separate measure 1−*DL* for both sensors, finally underestimating the BIL method. Similarity of NN and BIL contradicts the visual analysis (Figure 5). Using QNR it was found that NN as the worst method corresponds quite well to the JQM in this case.

In total it seems that both joint quality measures behave quite similarly except that QNR (1−*DL*) tends to underestimate BIL interpolation quality. Moreover, 1−*DL* measure appears to be more sensitive (exhibits higher variability) and 1−*DS* tends to be dependent on the sensor type.

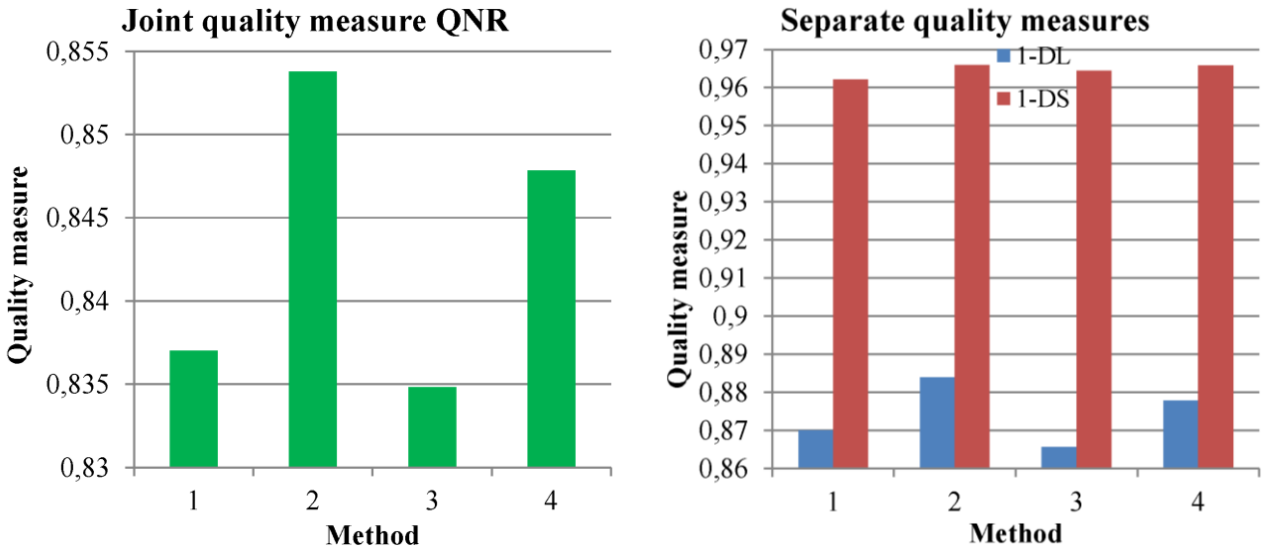

(**a**) (**b**)

Figure 4. QNR quality assessment of interpolation methods: 1—NN, 2—ZP, 3—BIL, and 4—CUB for WV-2 data. (**a**) QNR, (**b**) 1−*DL* and 1−*DS*.

(**a**) NN (**b**) ZP

Figure 5. *Cont.*

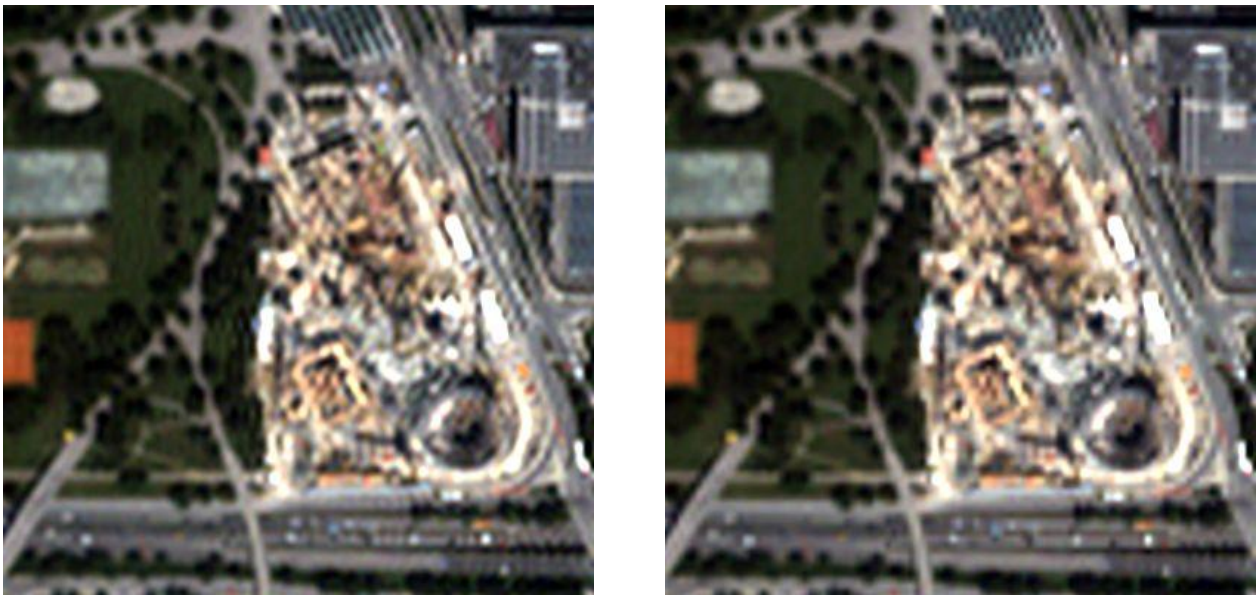

(**c**) BIL (**d**) CUB

Figure 5. Different interpolation methods: NN (**a**), ZP (**b**), BIL (**c**) and CUB (**d**) for the IKONOS data.

To enhance previously presented experiment, the separate quality measures 1−QLR and *DL* are additionally compared with two well established quality measures SAM (given in degrees) and ERGAS in Figure 6 for IKONOS data. Here, the low measure values stand for similar images. One can see that all measures, except *DL*, correlate quite well with each other (Figure 6a–c). Thus, a new measure QLR is legitimated for a practical usage in pansharpening quality assessment. The *DL* measure behaves unexpectedly for NN and ZP by underestimating the quality of NN and overestimating ZP. The reason for that can be the violation of the assumption about the preservation of between-band relations in different resolution scales. Similar results are observed for other experiments of this paper and sensor WV-2 data.

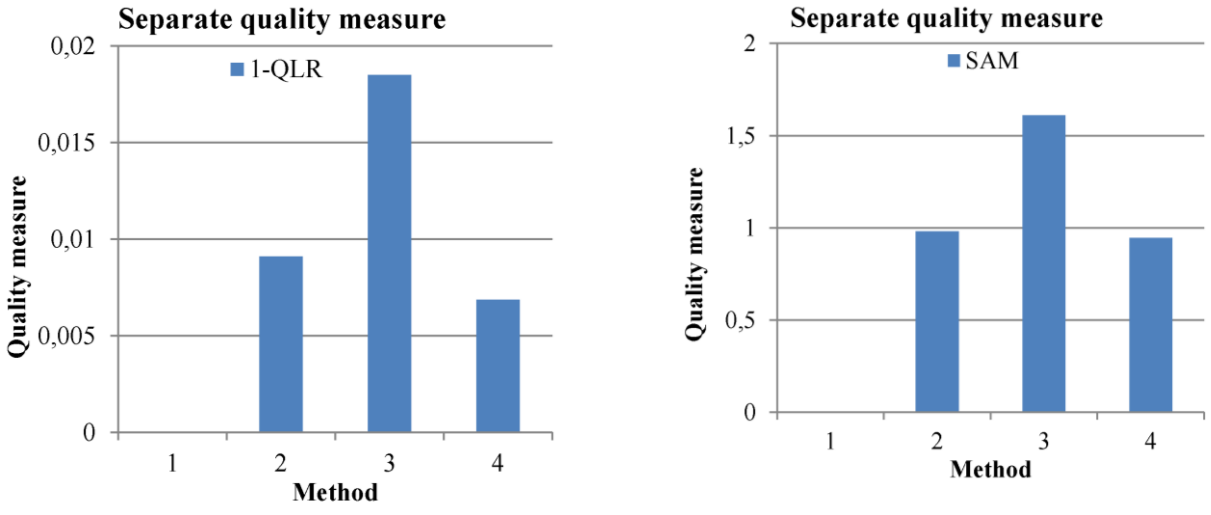

(**a**) (**b**)

Figure 6. *Cont.*

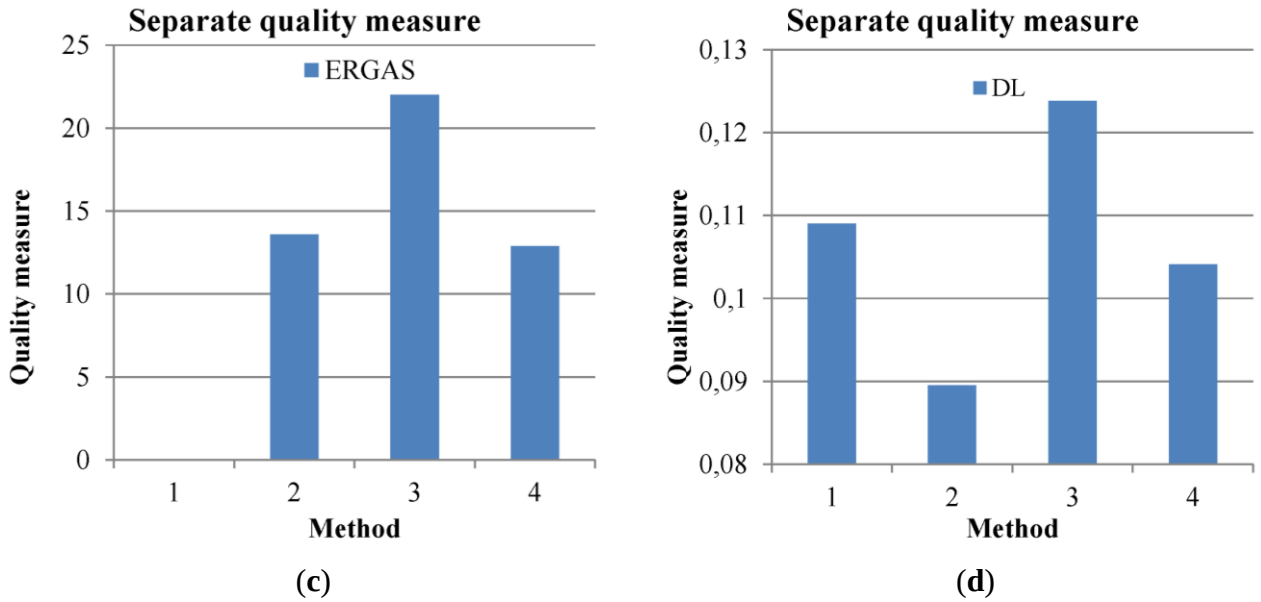

Figure 6. Quality assessment of interpolation methods: 1—NN, 2—ZP, 3—BIL, and 4—CUB for IKONOS data using different separate quality measures. (**a**) 1−QLR, (**b**) SAM, (**c**) ERGAS, (**d**) *DL*.

3.3. Interpolation Influence on the HPFM Pansharpening Method

The JQM quality of a selected pansharpening method using different interpolation methods is shown in Figures 7 and 8. In this case, the HPFM with a cutoff frequency 0.15 for IKONOS and WV-2 data is used.

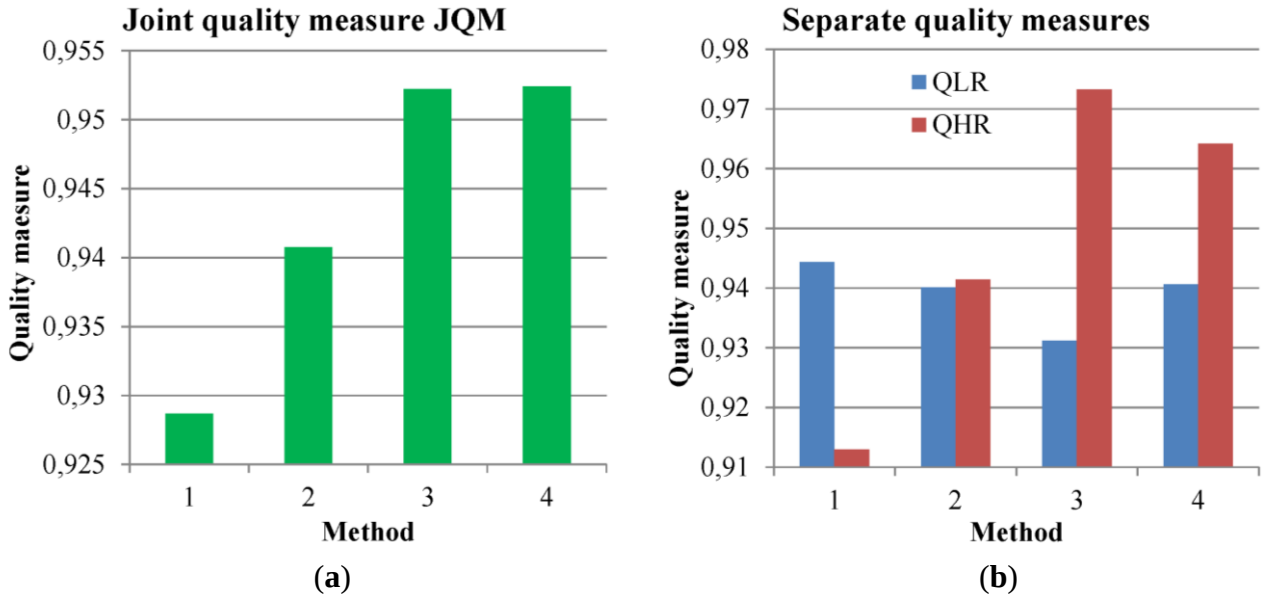

Figure 7. JQM quality assessment of High Pass Filtering Method (HPFM) for different interpolation methods: 1—NN, 2—ZP, 3—BIL, and 4—CUB for IKONOS data. (**a**) JQM, (**b**) QLR and QHR.

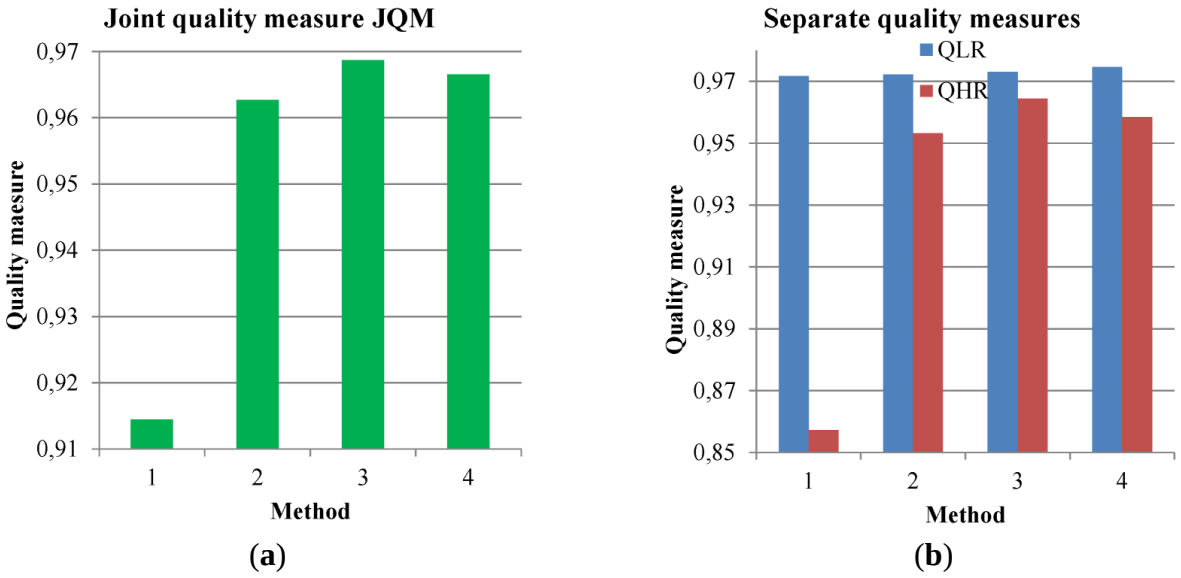

Figure 8. JQM quality assessment of HPFM for different interpolation methods: 1—NN, 2—ZP, 3—BIL, and 4—CUB for WorldView-2 data. (**a**) JQM, (**b**) QLR and QHR.

QLR is varying insignificantly for IKONOS (Figure 7b) and almost constant for WV-2 (Figure 8b) for all interpolation methods. From the point of view of QHR, NN is the worst method and BIL is better than the remaining two methods. These results lead to JQM (Figures 7a, 8a) ranking BIL as the best interpolation method for both sensors closely followed by CUB. NN is the worst of all interpolation methods. Thus, it seems that BIL is a suitable interpolation method regardless of sensor type and therefore only BIL interpolation is used in further experiments. The GFF method by definition only uses ZP interpolation method. For Ehlers fusion method, I have followed the recommendation to use CUB [24]. In ATWT implementation of [26], NN is used.

3.4. Comparison of Pansharpening Methods

The pansharpening methods and their parameter settings are listed in Table 2 ([21,22,24–26]), and the quantitative comparison results are presented in Figures 9 and 10.

Table 2. List of pansharpening methods.

Method	Cutoff Frequencies	Interpolation Method	Reference
1 GFF	0.05	ZP	[21]
2 GFF	0.15	ZP	[21]
3 GFF	0.3, 0.25, 0.25, 0.15	ZP	[21]
4 GFF	0.7	ZP	[21]
5 HPFM	0.05	BIL	[22]
6 HPFM	0.15	BIL	[22]
7 HPFM	0.3, 0.25, 0.25, 0.1	BIL	[22]
8 HPFM	0.7	BIL	[22]
9 CS IHS	-	BIL	-
10 CS GS	-	BIL	IDL ENVI 5.0
11 ATWT	-	NN	[25,26]
12 Ehlers	0.15, 0.15	CUB	[24]

The QLR measure behaves as expected for GFF (methods 1–4) and HPFM (methods 5–8) in dependence of the cutoff frequencies (Figure 9b). That is, QLR increases with the increase of cutoff frequency (spectral quality). QHR identifies methods 2 and 6 as the best, which correspond quite well with visual analysis in Figure 11d. For example, the image in Figure 11d exhibits much better spatial quality than the image in Figure 11f. Further, JQM selects methods 3 and 7 with band dependent cutoff frequencies (Figure 9a), which is well supported by visual interpretation in Figure 11. For example, the image in Figure 11e exhibits better spectral quality (e.g., compare with BIL in Figure 11a) than the image in Figure 11d simultaneously preserving good spatial quality. Moreover, it seems that HPFM, the faster variant of GFF, is better than GFF, maybe, due to the different interpolation method used. Thus, both measures QHR and JQM are able to correctly select optimal cutoff frequencies for both methods.

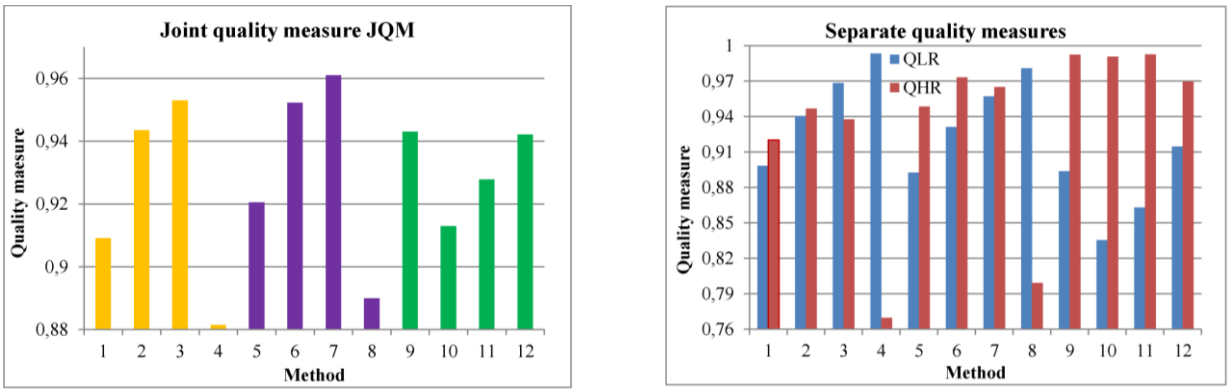

(**a**) (**b**)

Figure 9. JQM and separate measures for 6 methods and their different parameter settings for IKONOS data. (**a**) JQM, (**b**) QLR and QHR.

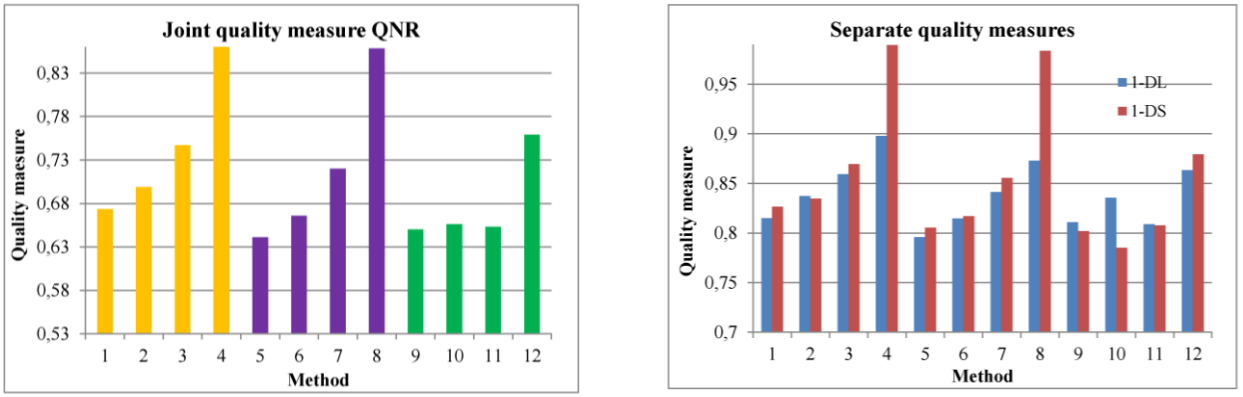

(**a**) (**b**)

Figure 10. QNR and separate measures for 6 methods and their different parameter settings for IKONOS data. (**a**) QNR, (**b**) 1−*DL* and 1−*DS*.

Spectral measure 1−*DL* follows approximately the behavior of QLR for methods 1–8 (Figure 10b). Spatial measure 1−*DS* again follows the trend of 1−*DL*, which contradicts visual analysis in Figure 11. An example is Figure 11f, the image with the estimated highest spatial quality exhibits in reality low quality when compared to Figure 11d,e. Such behavior of these two measures leads to the same trend of

the joint quality measure QNR in Figure 10a. Thus, QNR is not able to select optimal cutoff frequencies for GFF and HPFM methods.

QLR of other methods: CS IHS (method 9 in Table 2), CS GS (method 10), ATWT (method 11) and Ehlers (method 12) is lower than those of most filtering methods, whereas for QHR the opposite observation is valid. Finally, JQM of these methods 9–12 is lower than those of the best filtering methods 2–3, 6–7. For example, low JQM of method 10 is well illustrated visually in Figure 12. The colors of the image in Figure 12b are significantly different from those of BIL interpolation in Figure 11a or the best pansharpening method 7 in Figure 11e. QNR ranks methods 9–12 close to methods 1, 5 with high spatial quality. Only Ehlers (method 12) receives a high overall score.

(**a**) msi_k BIL

(**b**) *pan*

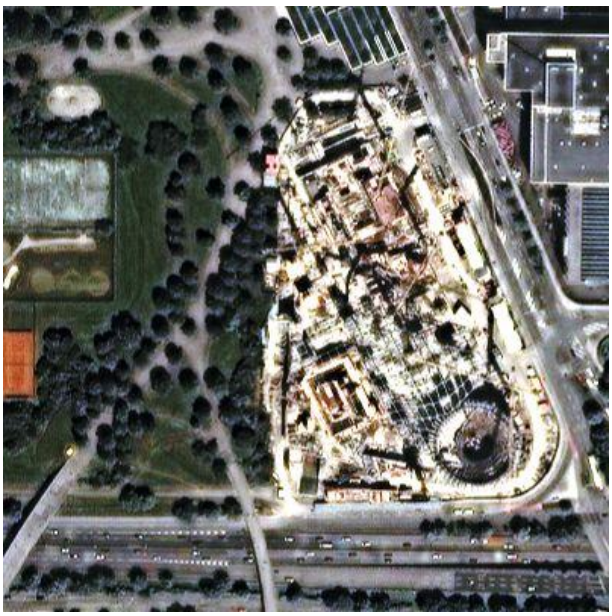

(**c**) HPFM 0.05

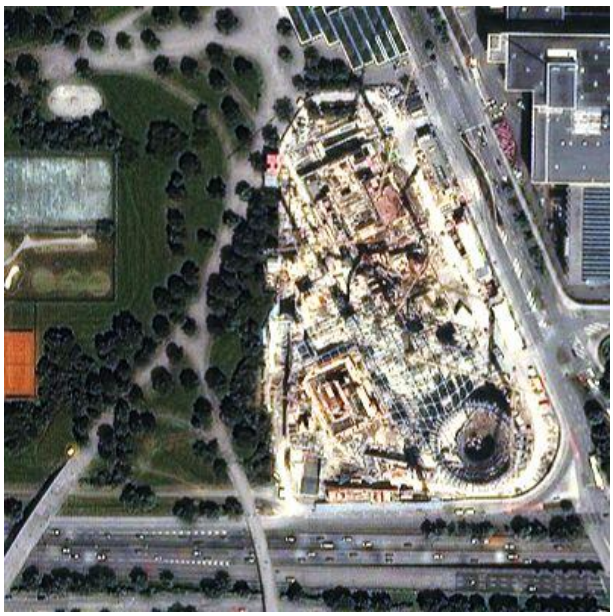

(**d**) HPFM 0.15

Figure 11. *Cont.*

(**e**) HPFM 0.3, 0.25, 0.25, 0.1

(**f**) HPFM 0.7

Figure 11. Bilinear interpolated bands: 3, 2, 1 (**a**), panchromatic band (**b**) and HPFM fusion with variable image quality controlled by parameters: 0.05 (**c**), 0.15 (**d**), band dependent parameters: 0.3, 0.25, 0.25, 0.1 (**e**) and 0.7 (**f**) for IKONOS data.

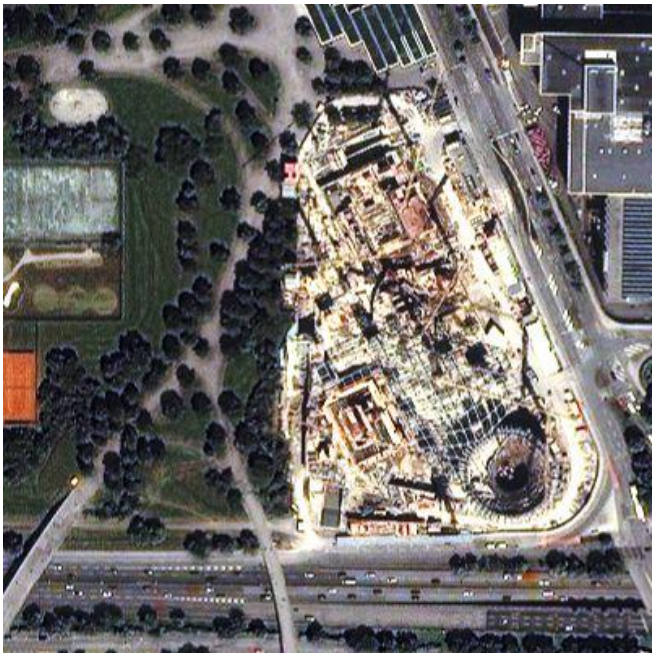

(**a**) CS IHS

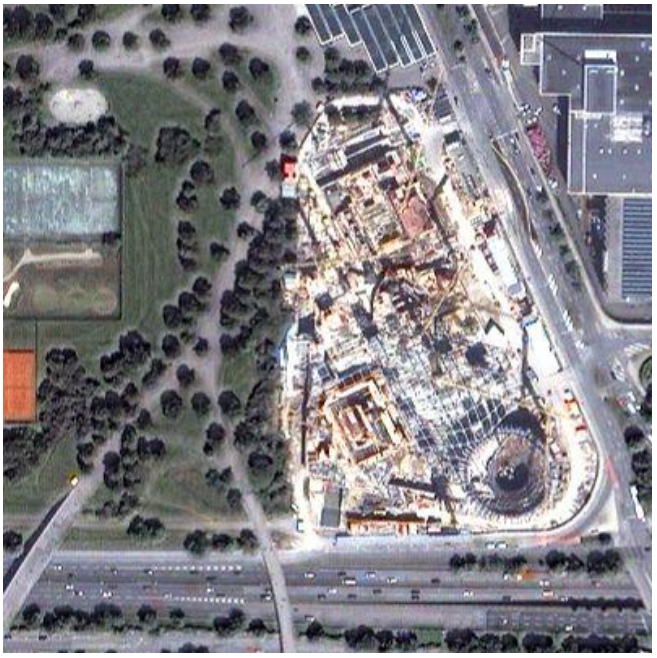

(**b**) CS GS

Figure 12. *Cont.*

(**c**) ATWT (**d**) Ehlers

Figure 12. Different fusion methods: CS IHS (**a**), CS GS (**b**), ATWT (**c**) and Ehlers (**d**) for IKONOS data.

In conclusion, I mention one more observation or drawback of QNR limiting its practical usage. JQM values of any pansharpening method (Figure 9a) are higher than those of only interpolation methods (Figures 1a, 3a). In contrast, QNR values of all interpolation methods (Figures 2a, 4a) are higher than these of all pansharpening methods (Figure 10a), except methods 4 and 8 whose quality as we know already is estimated wrongly.

4. Conclusions

The joint quality measure JQM is proposed, which is based on the new FR measure CMSC. The CMSC measure is translation invariant and thus can be preferable in applications such as classification, clustering, image matching and change detection requiring only the relative comparison of parameter values. JQM performs comparison of a fusion result separately (QLR and QHR) with each of the inputs of pansharpening. It allows practical selection of optimal filtering parameters and comparison of different pansharpening methods. The results are well supported by visual analysis and existing experience.

Already known QNR measure is based on the UIQI index, originally designed for visual perception tasks and thus can be preferable for visual evaluation of images or more generally scale invariant applications. Several unexpected properties of QNR are detected. It tends to underestimate the quality of BIL interpolation. Additionally, its spatial part $1-DS$ seems to be not able to correctly rank filtering based fusion methods in dependence of the filtering parameter. The quality of filtering methods for large parameter values is overestimated. Moreover, $1-DS$ overestimates the quality of all interpolation methods when compared with almost all fusion methods. Exceptions are filtering based methods with large parameters values, whose quality is again overestimated as already stated above. The cause of these

drawbacks of 1−*DS* can be its wrong/incorrect usage/definition. The bands with different spectral ranges (spectral inconsistency) are compared in this measure.

Future research could be directed towards a more comprehensive experimental investigation of quality measures on more data and various sensors. Further, the QNR measure can be enhanced by replacing UIQI with CMSC similarly as for JQM.

Acknowledgments

I would like to thank DigitalGlobe and European Space Imaging (EUSI) for the collection and provision of WorldView-2 scene over the Munich city.

Conflicts of Interest

The author declares no conflict of interest.

References

1. Yang, J.; Zhang, J. Pansharpening: From a generalized model perspective. *Int. J. Image Data Fusion* **2014**, *5*, 285–299.
2. Xu, Q.; Zhang, Y.; Li, B. Recent advances in pansharpening and key problems in applications. *Int. J. Image Data Fusion* **2014**, *5*, 175–195.
3. Pohl, C.; van Genderen, J. Structuring contemporary remote sensing image fusion. *Int. J. Image Data Fusion* **2015**, *6*, 3–21.
4. Alparone, L.; Wald, L.; Chanussot, J.; Thomas, C.; Gamba, P.; Bruce, L.M. Comparison of pansharpening algorithms: Outcome of the 2006 GRS-S data fusion contest. *IEEE Trans. Geosci. Remote Sens.* **2007**, *45*, 3012–3021.
5. Aiazzi, B.; Alparone, L.; Baronti, S.; Garzelli, A. Quality assessment of pansharpening methods and products. *IEEE Geosci. Remote Sens. Soc. Newsl.* **2011**, *161*, 10–18.
6. Makarau, A.; Palubinskas, G.; Reinartz, P. Analysis and selection of pan-sharpening assessment measures. *J. Appl. Remote Sens.* **2012**, *6*, 1–20.
7. Wald, L.; Ranchin, T.; Mangolini, M. Fusion of satellite images of different spatial resolutions: Assessing the quality of resulting images. *Photogramm. Eng. Remote Sens.* **1997**, *63*, 691–699.
8. Zhou, J.; Civco, D.L.; Silander, J.A. A wavelet transform method to merge Landsat TM and SPOT panchromatic data. *Int. J. Remote Sens.* **1998**, *19*, 743–757.
9. Alparone, L.; Aiazzi, B.; Baronti, S.; Garzelli, A.; Nencini, F.; Selva, M. Multispectral and panchromatic data fusion assessment without reference. *Photogramm. Eng. Remote Sens.* **2008**, *74*, 193–200.
10. Khan, M.M.; Alparone, L.; Chanussot, J. Pansharpening quality assessment using the modulation transfer functions of instruments. *IEEE Trans. Geosci. Remote Sens.* **2009**, *47*, 3800–3891.
11. Padwick, C.; Deskevich, M.; Pacifici, F.; Smallwood, S. WorldView-2 pan-sharpening. In Proceedings of ASPRS, San Diego, CA, USA, 26–30 April 2010; pp. 1–13.
12. Palubinskas, G. Quality assessment of pan-sharpening methods. In Proceedings of IGARSS, Québec, QC, Canada, 13–18 July 2014; pp. 2526–2529.

13. Wang, Z.; Bovik, A.C.; Sheikh, H.R.; Simoncelli, E.P. Image quality assessment: From error visibility to structural similarity. *IEEE Trans. Image Process.* **2004**, *13*, 600–612.
14. Palubinskas, G. Mystery behind similarity measures MSE and SSIM. In Proceedings of ICIP, Paris, France, 27–30 October 2014; pp. 575–579.
15. Zhu, X.; Milanfar, P. Automatic parameter selection for denoising algorithms using a no-reference measure of image content. *IEEE Trans. Image Process.* **2010**, *19*, 3116–3132.
16. Thomas, C.; Ranchin, T.; Wald, L.; Chanussot, J. Synthesis of multispectral to high spatial resolution: A critical review of fusion methods based on remote sensing physics. *IEEE Trans. Geosci. Remote Sens.* **2008**, *46*, 1301–1312.
17. Boggione, G.A.; Pires, E.G.; Santos, P.A.; Fonseca, L.M.G. Simulation of panchromatic band by spectral combination of multispectral ETM+ bands. In Proceedings of ISPSE, Hawaii, HI, USA, 10–14 November 2003; pp. 321–324.
18. Javan, F.D.; Samadzadegan, F.; Reinartz, P. Spatial quality assessment of pan-sharpened high resolution satellite imagery based on an automatically estimated edge based metric. *Remote Sens.* **2013**, *5*, 6539–6559.
19. Wang, Z.; Ziou, D.; Armenakis, C.; Li, D.; Li, Q. A comparative analysis of image fusion methods. *IEEE Trans. Geosci. Remote Sens.* **2005**, *43*, 1391–1401.
20. Aiazzi, B.; Baronti, S.; Lotti, F.; Selva, M. A comparison between global and context-adaptive pansharpening of multispectral images. *IEEE Geosci. Remote Sens. Lett.* **2009**, *6*, 302–306.
21. Palubinskas, G.; Reinartz, P. Multi-resolution, multi-sensor image fusion: General fusion framework. In Proceedings of JURSE, Munich, Germany, 11–13 April 2011; pp. 313–316.
22. Palubinskas, G. Fast, simple and good pan-sharpening method. *J. Appl. Remote Sens.* **2013**, *7*, 1–12.
23. Aiazzi, B.; Alparone, L.; Baronti, S.; Garzelli, A.; Selva, M. MTF-tailored multiscale fusion of high-resolution MS and Pan imagery. *Photogramm. Eng. Remote Sens.* **2006**, *72*, 591–596.
24. Klonus, S.; Ehlers, M. Image fusion using the Ehlers spectral characteristics preservation algorithm. *GISci. Remote Sens.* **2007**, *44*, 93–116.
25. Aiazzi, B.; Alparone, L.; Baronti, S.; Garzelli, A. Context-driven fusion of high spatial and spectral resolution images based on oversampled multiresolution analysis. *IEEE Trans. Geosci. Remote Sens.* **2002**, *40*, 2300–2312.
26. Canty, M.J. *Image Analysis, Classification and Change Detection in Remote Sensing: With Algorithms for ENVI/IDL and Python*, 3rd ed.; CRC Press: Boca Raton, FL, USA, 2014.